J Solid State Electrochem (2009) 13:591–598
DOI 10.1007/s10008-008-0694-0

ORIGINAL PAPER

Current pulse measurement of capacitance during molten salt electrochemical experiments

Graeme A. Snook · Katherine McGregor · Andrew J. Urban · Marshall R. Lanyon

Received: 31 July 2008 / Revised: 19 September 2008 / Accepted: 25 September 2008 / Published online: 16 October 2008

Abstract In earlier work in our laboratories, a current pulse method was developed that allows in situ (dynamic) measurements of electrode capacitance. The present work describes the successful application of the technique to the study of electrode properties in molten salt electrolytes. As expected, the electrode capacitance increases as the electrode surface area exposed to a molten salt bath increases. Furthermore, creep of the bath along the surface of a conductive ceramic anode and subsequent ingress into the anode pores is observed as an increase in capacitance. The pulse technique also gives an indication of phase changes that occur during the reduction of a solid titanium dioxide cathode and a highly sensitive measure of the temperature at which initial freezing of the calcium chloride electrolyte begins. These observations provide useful in situ information about changes in electrode properties in molten salt electrolytes that are difficult to obtain from other techniques.

Keywords Current pulse · Capacitance measurement · Molten salt electrochemistry · Resistometer · Solid-state electrochemistry · Resistance measurement · Electrowinning · Titanium

Introduction

The development of in situ techniques for studying molten salt electrometallurgy is essential for better understanding of the processes that occur in such systems. Processes that occur at the electrode surfaces cannot be easily observed during the course of an electrolysis performed in a conventional solid crucible and furnace. Consequently, it is often difficult to interpret changes in cell current and voltage and relate these unequivocally to electrode processes. These must be inferred upon completion of the electrolysis and removal of the electrodes from the cell. However, a wealth of information may be obtained from in situ dynamic capacitance measurements. In these laboratories, measurement of the dynamic cell resistance during molten salt electrowinning experiments has been made possible by the use of a purpose-built instrument known as a 'resistometer' [1–3]. Modification of this instrument has allowed capacitance measurements to be obtained simultaneously with resistance [3]. This instrument, first developed at CSIRO, works in conjunction with a potentiostat by applying an interrupted signal as a square, bipolar (typically 1 A) current pulse over a small time-scale (~210 μs) every 60 ms to measure the resistance [1, 3]. The pulse sequence is as follows: a 1 A pulse (70 μs duration); a rest period (70 μs duration); a reverse (−)1 A pulse (70 μs duration). A typical applied current pulse is shown in Fig. 1. As the pulse is bipolar, there is no net charge transfer. The principle is that a current pulse will cause a corresponding voltage pulse according to Ohm's Law:

$$V_{\text{pulse}} = I_{\text{pulse}} R_{\text{uncompensated}} \quad (1)$$

where V_{pulse} is the jump in voltage after application of the current pulse (I_{pulse}), from which the uncompensated resistance ($R_{\text{uncompensated}}$) can be calculated (see Fig. 1). The measurement is applied as a rapid, bipolar and relatively infrequently interrupted signal and consequently does not significantly disturb the Faradaic reactions or double-layer charging [1]. This measurement can be easily

For consideration in the Special Edition: Oldham Festchrift

Dedicated to our dear friend Keith B. Oldham on the occasion of his 80th birthday.

G. A. Snook (✉) · K. McGregor · A. J. Urban · M. R. Lanyon
CSIRO Minerals/CSIRO Light Metals Flagship,
P.O. Box 312, Clayton South, VIC 3169, Australia
e-mail: Graeme.Snook@csiro.au

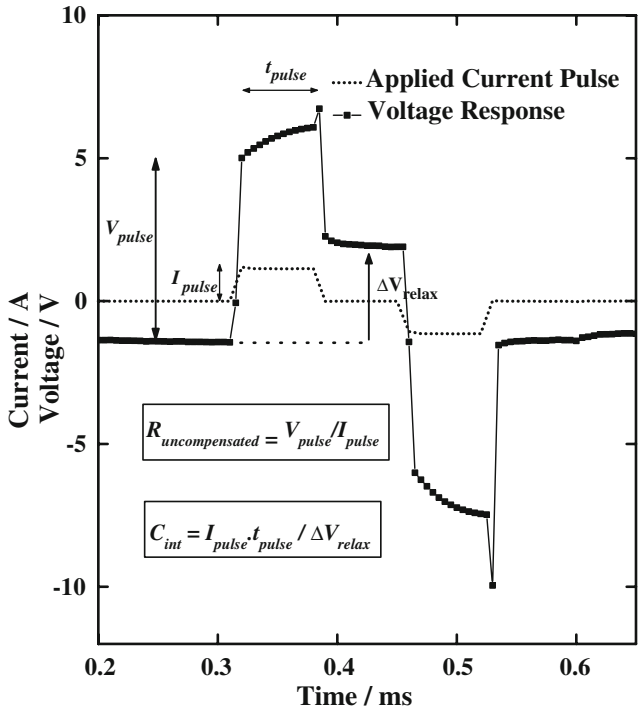

Fig. 1 In situ current pulse measurement of capacitance. Applied current pulse and corresponding voltage response with illustration of the measurement of resistance and capacitance

adapted to give capacitance as shown in Fig. 1. The capacitance is measured as [3, 4]:

$$C = I_{\text{input}} \Big/ \left(\frac{\Delta V_{\text{relax}}}{t_{\text{pulse}}} \right) \text{ or } C = \frac{I_{\text{input}} \cdot t_{\text{pulse}}}{\Delta V_{\text{relax}}} \tag{2}$$

where C is the capacitance, I_{input} is the current pulse magnitude (1 A), t_{pulse} is the time of the forward pulse (70 μs) and ΔV_{relax} is the voltage change from before the application of the pulse to during the rest period of the pulse (see Fig. 1).

If the counter electrode is sufficiently large, then the capacitance should be dominated by the response of the working electrode. The capacitance (C) is proportional to the area of this electrode exposed to the molten salt [5]:

$$C = \frac{\varepsilon A}{L} \tag{3}$$

Or

$$C = C_{\text{specific}} \times A \tag{4}$$

where ε is the permittivity, A is the area, L is the equivalent spacing of the capacitor plates (i.e. the double layer thickness), and C_{specific} is the specific capacitance.

In earlier work [3], we have tested the validity of this technique using a dummy cell (constructed using the Randles equivalent circuit) and adding varying amounts of capacitance. A series of electrochemical measurements in aqueous solution were also made, and the capacitance values obtained from the pulse current technique compare well with those obtained from cyclic voltammetry and AC impedance spectroscopy. Finally, the application of the method in a molten salt environment was evaluated, and the results demonstrated that the current pulse method gave a high frequency component of the capacitance accurately (equivalent to ~2–14 kHz). The capacitance values obtained from the pulse current technique described here will depend on the sum of all the capacitances active in this frequency range, including those due to the double layer, impurity adsorption, charge transfer, corrosion, etc. That is, they are not a true double layer capacitance. This interpretation is supported by a recent study by Kisza [6]. Nonetheless, the measurements allow changes in the active electrode area exposed to the molten salt bath to be measured, e.g. if surface oxides are formed on the electrode, then a change in C_{specific} will be seen, or if the electrode is consumed or falls apart during electrolysis, this will be observed as a rapid drop or change in capacitance.

The in situ capacitance measurements should reveal many interesting phenomena when applied to the investigation of electrode properties in molten salt or ionic liquid environments [6–11].

Experimental

Electrochemical measurements were performed using an EG&G PAR Model 362 scanning potentiostat and an EG&G PAR Current Booster Model 365 (10 A). Experimental details for the furnace, cell and calcium chloride bath preparation are given in [12]. A schematic diagram of the laboratory cell is shown in Fig. 2. All measurements were performed in two electrode mode (without a reference electrode) either at open circuit, or using galvanostatic control (1 A). The oversized TiO_2 cathode was prepared by spotwelding a small piece of Kanthal strip to a length of Kanthal wire (18 gauge) and pressing the strip into a sintered alumina dish (60 mm diameter). A slurry of titania paste, 40 g, prepared from TiO_2 (99.5%, minimum purity rutile, Alfa Aesar) and deionised water, was added to the dish, covering the Kanthal strip and oven-dried for 24 h. The Kanthal wire was sheathed with a sintered alumina rod to prevent corrosion and attack by the calcium chloride bath. The cathode assembly was placed at the bottom of an alumina crucible. Three types of anodes were used in the experiments: a copper rod (3.3 mm diameter); a rectangular ceramic bar (8.84×4.37 mm); or a graphite rod (POCO graphite, 10 mm diameter). The depth required to dip the

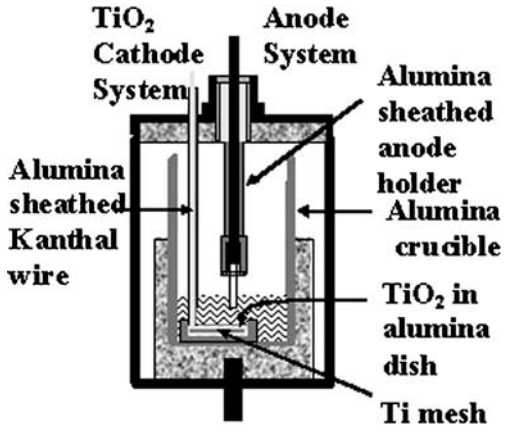

Fig. 2 Experimental setup for a typical high temperature molten salt TiO_2 reduction experiment

electrodes was calculated using a so-called copper dip test. This involved dipping a copper rod into the bath and marking the top of the furnace port on the rod and removing the rod. This is done rapidly enough, such that the $CaCl_2$ freezes onto the rod, allowing measurement of the depth of the molten salt bath and the distance from the top of the furnace port to the top of the bath. Absolute measurement of when the anode was touching the top of the molten salt bath was done by measuring the cell resistance while lowering the anode while the cell was at open circuit. This resulted in the cell resistance changing from well in excess of 10 Ω to below 10 Ω (within the measuring range of the resistometer). The upper part of a copper rod was sheathed with an alumina tube and the exposed part lowered into the bath while electrically connected to the potentiostat and resistometer. The POCO graphite rod and the ceramic anode were both attached to an alumina sheathed stainless steel rod.

An in-house built resistometer [1] was connected between the potentiostat and the cell to supply an interrupted current pulse signal (every 60 ms) of 1 A (70 μs duration) followed by a rest period (70 μs duration) and reverse (−)1 A pulse of the same duration. The current pulse signal (between working electrode and ground) was passed through a Schmidt trigger and used to trigger the logging of the pulse data. National Instruments Labview version 7 software in combination with a National Instruments SCB-68 terminal box and NI6036 multi-function data acquisition board was used to capture 20 signals (typically sampled at 200 kHz) and average the signals (every 2 s) to give an average voltage response between the working electrode and the reference electrode terminals on the resistometer. The Labview programme generated the capacitance measurement together with the resistance and cell voltage.

Results and discussion

Copper rod dip tests at open circuit

Using a $CaCl_2$ bath (950 °C) and an oversized pasted titania cathode (~40 g TiO_2), the effect of dipping a copper anode (3.3 mm diameter) to depths between 0 to 30 mm into the molten salt bath is measured [3, 12]. If the titania electrode is sufficiently oversized, the capacitance will be dominated by the anode. Since the cathode has a geometric area of ~28 cm^2 exposed directly the bath (and considering that the pasted electrode is at least 10 mm thick) it is most likely this electrode is considerably oversized. This means that, if the rod is dipped to different depths, the capacitance measured should scale with the depth of the dip (d) as the area exposed to the electrolyte will scale linearly with this depth:

$$A = \pi r^2 + d(2\pi r) \tag{5}$$

where A is the area, r is the radius of the rod (1.65 mm).

Figure 3 shows the linear relationship between the measured capacitance (via the pulse method) and the dip depth. The first point on the graph (just touching the rod on the bath surface) is determined using the resistometer. This is the point at which the resistance changes from a large value to a value below 10 Ω. The errors given in the graph are from the calculated standard deviation from 20 collected signals. Using the area calculated and the capacitance value, the copper was found to have a specific capacitance of around 3.5±0.4 mF cm^{-2}. This calculation uses the geometric surface area and does not take into account the porosity and its effect on true surface area. This specific capacitance compares well with an example of platinum in

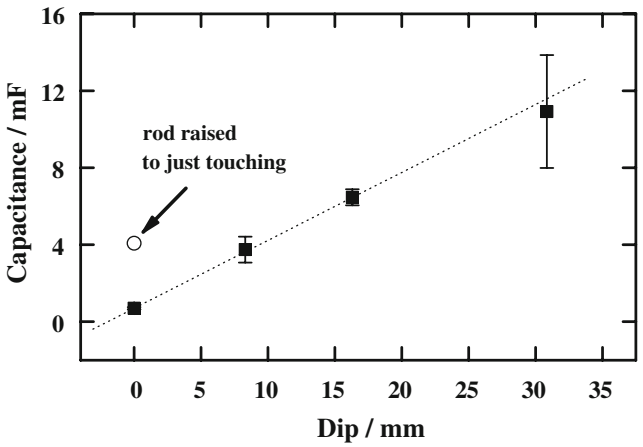

Fig. 3 Capacitance measured from the current pulse measurement for a copper rod (3.3 mm diameter) dipped in a $CaCl_2$ bath (950 °C) to different depths using an oversized titania (~40 g) cathode

molten $(Li/K)_2CO_3$ of 4.13 mF cm^{-2} obtained via AC Impedance measurements [13]. In both the present study and the value quoted from [13], the measured capacitance is not a true double layer capacitance (which is in the tens to hundreds of microfarad range) but includes a component of corrosion capacitance (essentially a Faradaic pseudo-capacitance from a slow interaction of the copper rod with the calcium chloride bath). This interpretation is supported by a recent study of capacitance and the double layer by Kisza [6]. The corrosion capacitance (or pseudocapacitance) appears to be constant over the time-frame of the pulse measurement (5 min), i.e. no significant physical change to the surface of the copper electrode is observed during this time. At the end of the measurement, the rod is raised back to where it just touches the bath surface (first position), and the capacitance lowers to the value indicated in Fig. 3 (~4 mF), which is not quite back to the original capacitance (~1 mF) as some of the electrolyte may not have drained entirely from the electrode, or slight corrosion of the copper rod has occurred. Nevertheless, the results suggest that the cathode and anode surfaces have not changed significantly due to dipping in the molten salt bath or due to the application of the current pulse at open circuit potential. Also, for a repeat measurement, with a fresh oversized cathode, the calculated specific capacitance is: 3.8±1.0 mF cm^{-2}.

During the capacitance measurements at open circuit, the current pulse is so rapid that no *significant* Faradaic reactions occur, such as the reduction of the TiO_2 cathode to Magnéli phases. This is shown by the return of capacitance to near the original value when raising the copper rod. Capacitance measurements were also obtained following a 10-min constant current electrolysis (where there is some conversion of TiO_2 cathode material), and these values were appreciably larger than the values found from the open-circuit measurements (see "Observation of capacitiance on a graphite anode during reduction of solid TiO_2"). Assuming a capacitance of around 1 mF, the Faradaic resistance must be below ~100 mohms (i.e. an extremely fast Faradaic reaction), in order to see the reaction on the 70 μs timescale. Consequently, the pulse is too fast to drive any significant Faradaic reactions at the cathode. However, it is slow enough to be affected by the relatively rapid corrosion of the copper rod (which occurs at open circuit due to reaction with the calcium chloride bath). The bipolar nature means that the anodic charge and the (cancelling) cathodic charge are injected into the system before the electrochemistry can react. In technical terms, due to the relationships $Z=1/j\omega C$ and $C=\varepsilon A/d$, the impedance (Z) is small at large area (A). Therefore, the capacitive impedance of the counter electrode (large A) is negligible at high frequencies (microsecond timescale) due to its large area. Therefore at ultra-short times (i.e. high frequencies) the counter electrode makes no contribution to the impedance of the cell.

Observation of creep on conductive ceramic anodes at open circuit

We have observed a significant amount of electrolyte creep along the surface of conductive ceramic inert anodes during titanium electrowinning studies, using a Fray–Farthing–Chen type process [12, 14]. The relevant reactions are given below:

Cathode reaction:

$$TiO_2(s) + 4e^- \rightarrow Ti(s) + 2O^{2-}$$

Anode reaction:

$$2O^{2-} \rightarrow O_2(g) + 4e^-$$

Overall reaction:

$$TiO_2(s) \rightarrow Ti(s) + O_2(g)$$

This creep changes the effective surface area of the electrode and can cause substantial corrosion and eventual failure of the electrode holder. Consequently, understanding when creep occurs and to what degree it occurs is important. The problem with conventional molten salt measurements is that creep cannot normally be observed unless a see-through (transparent) cell is utilised. The evidence for electrolyte creep is usually obtained from ex situ analysis of the electrode upon its removal from the cell.

An extra complication is the inability to observe the electrode when immersing it to a specified depth in the bath (the electrode is lowered into a solid alumina crucible within a vertical tube furnace). This can lead to errors in the immersion depth, estimated to be ±2 mm, and is discussed in more detail in the analysis of the capacitance data.

Prior to electrolysis, the ceramic anode is soaked for 1 h in a calcium chloride bath at open circuit and then the electrolysis proceeds for periods of up to 50 h [12]. Figure 4 shows photographs of two typical ceramic anodes at the completion of an electrolysis. It can be seen that the actual electrolyte level exposed to the bath is much higher than the original immersion depth. The question is—when does this creep occur? Is it rapid or does it occur gradually through the experiment?

Using a combination of the 'copper dip test' and the 'resistometer dip test', the ceramic electrode (dimensions 8.84×4.37 mm) is immersed to a depth of 9±2 mm and soaked in a calcium chloride bath for 1 h. Figure 5 shows the measurements of resistance and capacitance during this time. The capacitance starts at a low value of ~0.8 mF, and the cell resistance starts at ~3.3 ohm. In earlier work, we have established that whilst a significant amount of this

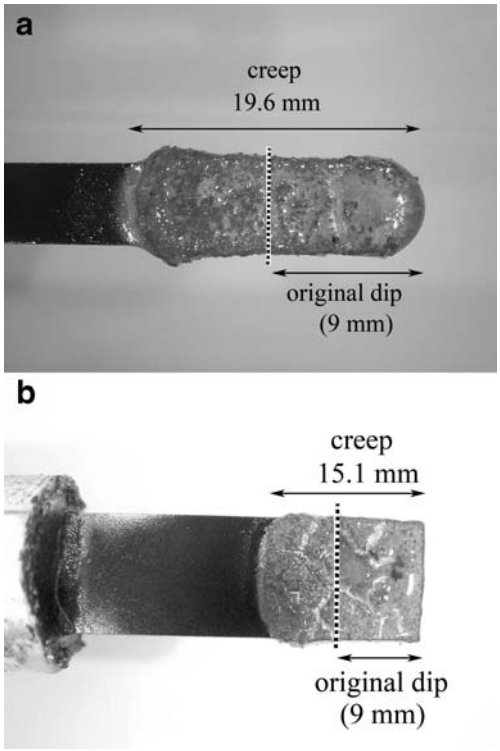

Fig. 4 Photographs of conductive ceramic anodes once cooled and removed from the furnace after a 24–50-h electrolysis run

resistance (~1 ohm) originates from the ceramic anode, the majority of the resistance (~ 2 ohm) is due to the oversized pasted TiO_2 cathode (McGregor et al. 2005). During the soaking step at open circuit, the cell resistance falls slightly from ~3.3 to ~2.8 ohm (due to a greater electrode surface area exposed to the electrolyte), whereas the capacitance increases by a factor of 2.5 (for the same reason). It appears that the capacitance value is a more sensitive measure of the active area. After an hour, the capacitance appears to plateau, which suggests that the source of the increase in capacitance reaches equilibration in about 1 h. It is most likely that this increase in anode capacitance is due to electrolyte creep and that the majority of it occurs in the first hour of soaking.

To support the hypothesis that this is due to electrolyte creep, a calculation of the change in electrode area exposed to the electrolyte is performed. When the electrode is removed from the experiment, the measured dip depth (similar to that observed in Fig. 4) is found to be 19 mm, which corresponds to a surface area of 5.41 cm^2. If the electrode is assumed to be immersed accurately to the target depth (9 mm), the area exposed is 2.76 cm^2. Assuming that negligible creep occurs after the initial soaking time, the area exposed to the electrolyte has increased by a factor of 1.96. This is close to the factor by which the capacitance has increased (i.e. 2.5). The factor could be slightly low because the actual dip may have been slightly lower than 9 mm, for reasons explained earlier. The other explanation for a slightly higher capacitance change than expected is that there is a certain degree of ingress of electrolyte into the pores of the electrode (ceramic anode density, ~97%.)

In a separate set of experiments, a thinner ceramic anode rod was used (5.32×3.56 mm). This time, the capacitance changed in the first hour from 0.94 to 1.29 mF which is a ratio of 1.37. Again, the initial target depth was 9±2 mm (1.79±0.35 cm^2), and the final measured depth this time was 15.5 mm (2.94 cm^2) giving a ratio of 1.64. This corresponds to an actual initial dip depth of 11 mm (2.14 cm^2), which lies within the estimated range.

Observation of capacitance on a graphite anode during reduction of solid TiO2

A series of measurements were also performed during the galvanostatic reduction of TiO_2 to titanium metal using a

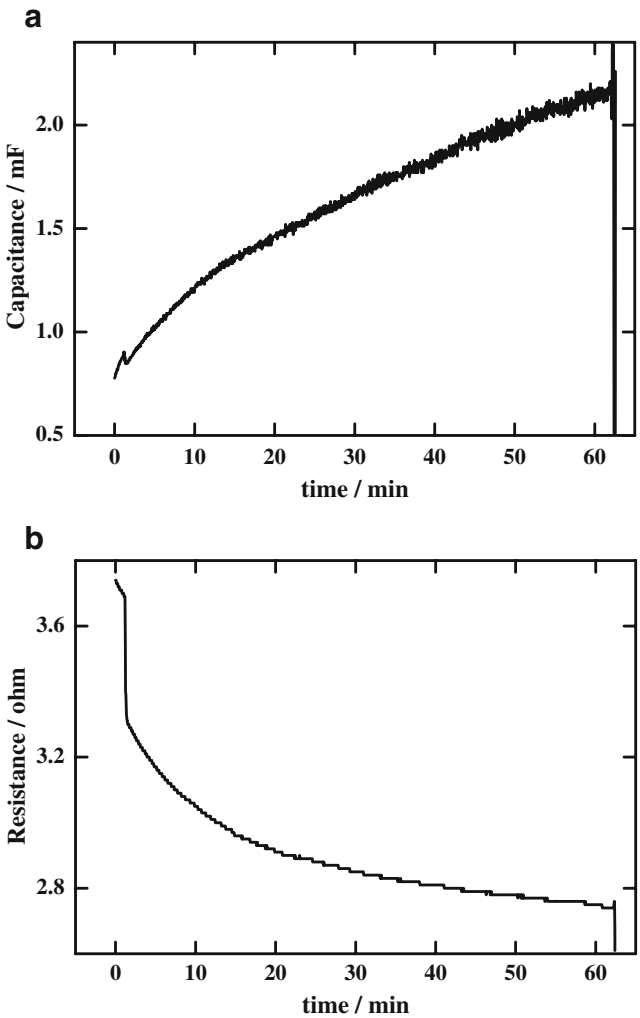

Fig. 5 **a** Capacitance observation of creep on a ceramic anode during the first hour of soaking; **b** resistance measurement

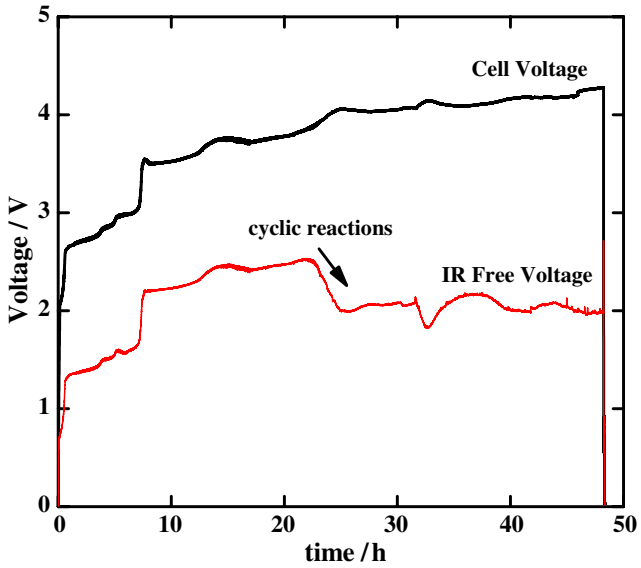

Fig. 6 Cell voltage and IR-free voltage for a constant current electrolysis run (1 A, ~48 h) using a POCO graphite anode and oversized, pasted TiO_2 cathode

consumable graphite anode (POCO graphite). The relevant reactions are given below [14]:

Cathode reaction:

$$TiO_2(s) + 4e^- \rightarrow Ti(s) + 2O^{2-}$$

Anode reaction:

$$C + 2O^{2-} \rightarrow CO_2(g) + 4e^-$$

Overall reaction:

$$TiO_2(s) + C \rightarrow Ti(s) + CO_2(g)$$

The graphite rod was immersed to a target depth of 35± 2 mm, with no appreciable soak time. Previous observations have shown that negligible creep occurs on this material during electrolysis. The measured depth of bath observed on the electrode was 33.6 mm (ex situ observation). Figure 6 shows both the cell voltage and the IR-free voltage for the constant current (1 A) electrolysis. The IR-free voltage (obtained by subtracting the *IR* value from the cell voltage) is an accurate measure of the potential required to maintain the electrochemical reduction reaction. The voltage goes through a series of increasing plateaus that correspond to the conversion of TiO_2 to various reduced forms (intermediates in the eventual process of full reduction to titanium metal such as the Magnéli phases Ti_nO_{2n-1}, Ti_2O_3, Ti_3O_5, TiO, Ti_2O, etc.; McGregor et al. 2005) [15]. The voltage plateaus begin to decrease in value at times after 20 h due to cyclic side reactions that occur in the bath and produce side products such as carbonates and carbides [16–19]. The initial slow voltage increase in the first 500 s of electrolysis is due to the initial slow ramping of current to 1.0 A at 2 mA/s.

Having understood some of the reactions that occur in this electrolysis, we can look at the capacitance and resistance responses. Firstly, it must be understood that with this measurement, a large graphite electrode is used (~27 cm^2 geometric area), and consequently, changes in capacitance of both the electrodes (graphite and TiO_2) will be significant. Figure 7 shows these responses in the first 30 min of the experiment. Initially, the graphite rod is lowered slowly into the bath. At time zero, the graphite rod is just touching the molten salt bath. It is lowered in three stages to the final point at ~8 min at which time the current ramp is applied. The capacitance increases and the cell resistance decreases, as the rod is lowered.

Figure 7 shows that during the first 25 min of the electrolysis, the cell resistance is fairly invariant, but the capacitance rapidly changes from ~0.4 to 3 mF (a factor of 8). Titania is known to form highly conducting and highly capacitive reduced phases (so-called Magnéli phases) during the early stages of electrolysis [12]. This could account for the rapid change in capacitance. There will be some variation in capacitance with potential during the measurement; this is well known in the literature [7, 11]. However, the large increase is more likely to be due to the

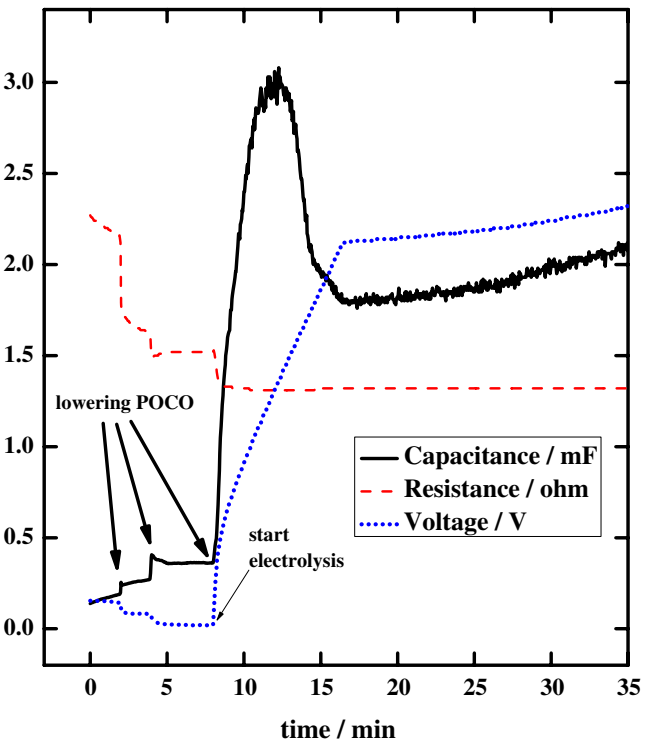

Fig. 7 Capacitance, resistance and voltage plots for the same electrolysis run in the first half hour

increase in (Faradaic) pseudo-capacitance of the titania cathode due to the changes in phase composition. It is likely that both the titania and the graphite electrodes will influence the capacitance (e.g. lowering of the graphite rod increased the capacitance by a factor of ~2). The rapid change in capacitance could be attributed to roughening of the graphite surface as CO_2 gas is evolved. Intriguingly, the capacitance reaches a peak and settles to a lower value once the maximum current is achieved and the voltage increase has finished.

On the longer timescale (Fig. 8), there are numerous changes in voltage associated with the reduction of TiO_2. The first of these voltage changes (A) results in a major change in capacitance from ~3 to ~16 mF. Again, the response is peaked. This could be due to the more highly conducting phases of reduced TiO_2 that are formed. The next two processes (B) show an increase in resistance but only minor changes in capacitance. This suggests the next processes form less conducting and slightly less capacitive phases. The next voltage plateau change is very major (C) and again causes a large change in capacitance as does the next voltage change (D). The final voltage response (E), beyond 20 h, involves the cyclic reactions and the capacitance eventually lowers to a very low value (~0.23 mF). This is associated with a large change in resistance.

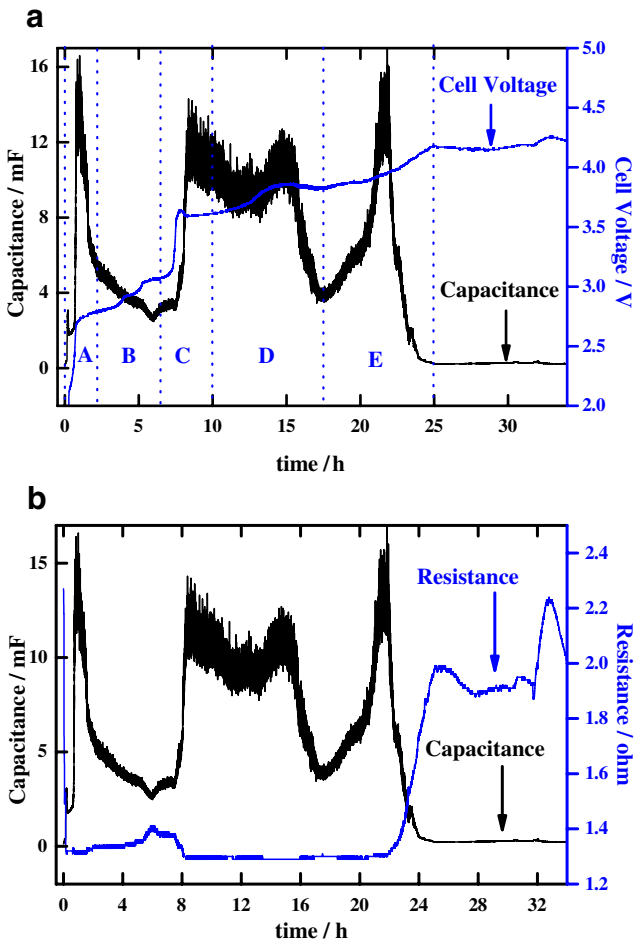

Fig. 8 **a** Capacitance and cell voltage for the first 34 h of a constant current electrolysis run (1 A) using a POCO graphite anode and oversized, pasted TiO_2 cathode; **b** Capacitance and resistance

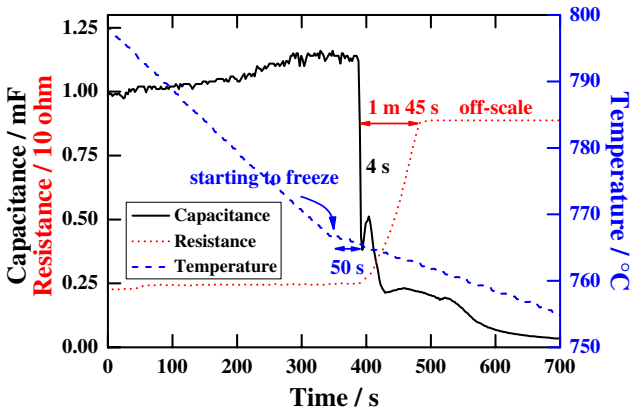

Fig. 9 Observation of freezing of the $CaCl_2$ electrolyte using bath temperature, resistance and capacitance measurements. A POCO graphite anode (dipped to 15 mm) and oversized TiO_2 pasted cathode were used

So, the in situ capacitance measurements can give an indication of electrode phase changes that occur during molten salt electrolysis, e.g. the reduction of solid TiO_2 in a chloride bath. Further work, though, is required to fully characterize or assign the complex processes observed in Fig. 8.

Observation of freezing of a molten salt electrolyte

We are also interested in detecting the initial freezing of the molten salt bath following the electroreduction of solid-state metal oxides to their metals, e.g. titanium dioxide (TiO_2) to titanium metal. Such metals are often highly reactive, and back reactions with any adventitious impurities present (e.g. oxygen) are undesirable. At the end of the electrolysis, however, if the current flow is maintained while the bath is cooling until it just reaches its freezing point, this inhibits back reactions and gives a more pure metal product [20]. Measurement of the capacitance should provide rapid detection of the initial freezing of the molten salt electrolyte, more rapid than resistance measurements. As the melt freezes, the resistance increases somewhat slowly but does not show a clear transition for freezing as there are still small pathways of molten electrolyte in the cooling bath. The capacitance (a surface phenomenon), however, will change rapidly as the interface between the electrolyte and the electrode freezes.

The final experiment involves observation of freezing of a $CaCl_2$ bath. In this study, a graphite electrode was

immersed to a bath depth of 15±2 mm (TiO_2 cathode is oversized for this experiment) and a small amount of electrolysis was carried out to steady the capacitance at around 2 mF. The furnace was switched off, and the temperature of the bath was measured using an alumina sheathed thermocouple dipped into the top of the bath. Initially, as the bath cooled, the capacitance dropped from 2 to ~1 mF (from 960 to 840 °C) but steadied at 1 mF before freezing occurred. This drop in capacitance with temperature is predicted from theory and has been observed by other workers [21–23]. This trend is opposite to that seen in aqueous electrolytes and other solvents. Figure 9 shows the last stages of cooling, in which the bath fully freezes. The rate at which the temperature of the bath (right axis) drops with time slows at the freezing point due to latent heat. A further 50 s later, the capacitance changes rapidly from ~1 to ~0.3 mF in only 4 s. The interface of either or both electrodes must change rapidly on freezing. This measurement of capacitance indicates the point of initial freezing. It takes a further 1 min and 45 s to dramatically affect the resistance and cause the measurement to go off scale. This measurement of resistance indicates the point of final freezing. This is a fascinating observation of freezing phenomena in the molten salt bath. Use of the technique has helped improve the quality of the titanium metal obtained from sintered TiO_2 pellets in our laboratories.

Concluding remarks

The in situ capacitance measurements provide a powerful technique for observing changes in electrode properties during molten salt electrolysis. Relative electrode area exposed to the bath is observed through copper dip tests and creep tests on a ceramic anode. A series of phase changes are observed during the reduction of a TiO_2 cathode in a calcium chloride bath. Finally, the subtleties of freezing of a calcium chloride bath are observed through the dynamic measurement of capacitance along with the measurement of resistance. The results described here demonstrate that the in situ capacitance measurements obtained from the pulse current technique are a highly sensitive measure of changes to the physicochemical environment of the electrode surface. As such, we plan to employ this technique for further studies of systems where electrode surface effects are important, e.g. in the study of the 'anode effect' in aluminium smelting cells which is usually caused by the temporary formation of an insulating bubble layer on the anode surface.

Acknowledgements This work was conducted as part of the CSIRO Light Metals Flagship.

The authors would like to thank their colleagues Mr. John Hamilton for construction of the resistometer and assistance in obtaining accurate voltage and current measurements, Dr. Noel Duffy for useful discussions and Mr. Mike Horne and Dr. Tony Hollenkamp for most constructive comments on the manuscript.

References

1. Deutscher RL, Fletcher S, Hamilton JA (1986) Electrochim Acta 31:585. doi:10.1016/0013-4686(86)85037-X
2. Fletcher S (1993) J Chem Soc Farad T 89:311. doi:10.1039/ft9938900311
3. Snook GA, Urban AJ, Lanyon MR, McGregor K (2008) J Electroanal Chem 622:225. doi: 10.1016/j.jelechem.2008.06.010
4. Monakhov VV, Utkin AB (1999) Tech Phys 44:342. doi:10.1134/1.1259336
5. Oldham KB, Myland JC (1994) Fundamentals of Electrochemical Science. Academic, New York
6. Kisza A (2006) Electrochim Acta 51:2315. doi:10.1016/j.electacta.2005.03.093
7. Kisza A (2002) J Electroanal Chem 534:99. doi:10.1016/S0022-0728(02)01148-8
8. Kisza A, Kazmierczak J, Meisner B (2004) Pol J Chem 78:1235
9. Kisza A, Kazmierczak J, Meisner B (2004) Pol J Chem 78:561
10. Oldham KB (2008) J Electroanal Chem 613:131. doi:10.1016/j.jelechem.2007.10.017
11. Graves AD, Inman D (1970) J Electroanal Chem 25:357. doi:10.1016/S0022-0728(70)80098-5
12. McGregor K, Frazer EJ, Urban AJ, Pownceby MI, Deutscher RL (2006) ECS Trans 2:369. doi:10.1149/1.2196026
13. Zeng CL, Wang W, Wu WT (2001) Corros Sci 43:787. doi:10.1016/S0010-938X(00)00108-6
14. Chen GZ, Fray DJ, Farthing TW (2000) Nature 407:361. doi:10.1038/35030069
15. Dring K, Hagen E, Lorentsen O and Rosenkilde, Patent Number: WO2007145526
16. Fray DJ (2002) Can Metall Q 41:433
17. Pistorins PC, Fray DJ (2006) J S Afr Inst Min Metall 106:31
18. Xu Q, Deng LQ, Wu Y, Ma T (2005) J Alloy Comp 396:288. doi:10.1016/j.jallcom.2005.01.002
19. Xu S, Melendres CA, Park JH, Kamrath MA (1999) J Electrochem Soc 146:3315. doi:10.1149/1.1392473
20. Chen GZ, Fray DJ, Farthing TW (2001) Metall Mater Trans B 32:1041. doi:10.1007/s11663–001–0093–8
21. Boda D, Henderson D, Chan KY (1999) J Chem Phys 110:5346. doi:10.1063/1.478429
22. Reszko-Zygmunt J, Sokolowski S, Henderson D, Boda D (2005) J Chem Phys 122:084504. doi:10.1063/1.1850453
23. Reszko-Zygmunt J, Sokolowski S, Pizio O (2005) J Chem Phys 123:016101. doi:10.1063/1.1949209